Full Paper Transactions, SMiRT 28
Toronto, Canada, August 10-15, 2025

SEISMIC NONLINEAR SSI STUDY FOR DEEPLY EMBEDDED SMR UNDER COHERENT AND INCOHERENT WAVES FOR DEEP SOIL SITE

Dan M. Ghiocel [1]

[1] Ghiocel Predictive Technologies, Rochester, New York, USA (dan.ghiocel@ghiocel-tech.com)

ABSTRACT

The paper investigates the nonlinear soil-structure interaction (SSI) analysis effects on a typical deeply embedded Small Modular Reactor (SMR) structure subjected to severe seismic excitations including both coherent and incoherent soil motions. The paper investigation is an extension of a research study based on linearized SSI analysis based on the ASCE 4-16 standard guidelines (Ghiocel and Todorovski, 2025). In this paper, the focus is on the nonlinear structure SSI modeling and dynamic behavior for the deeply embedded SMR structure is investigated in the light of standard and regulatory requirements in US and Japan. The nonlinear SSI approach is based on highly efficient, highly practical hybrid frequency-time approach. The iterative approach is fast converging in only few SSI restart iterations. In addition to the nonlinear structure behaviour, the nonlinear wall-soil interface slipping effects are also considered. Comparative nonlinear SSI responses include ISRS and structural forces in the SMR walls for coherent and incoherent motions based on the best engineering practices for structural modeling in US and Japan. The ACS SASSI Option NON software was used for SSI analyses.

NONLINEAR SSI METHODOLOGY

The applied nonlinear SSI methodology is based on highly practical, efficient hybrid approach that uses an iterative scheme, which couples the equivalent-linear complex frequency SSI analysis with a fast nonlinear time-domain hysteretic analysis using a structure reduced-order modelling. The reduced-order modelling uses macro-mechanics models for idealization RC or SC structure wall behaviour (Ghiocel et al., 2022a, 2022b). The iterative SSI approach which was implemented in ACS SASSI Option NON (Ghiocel Predictive Technologies, 2024) is fast converging in only few SSI restart iterations. The nonlinear SSI approach implementation follows conceptually the Japanese structure modelling and seismic engineering practices. Specifically, the implementation is compliant with the nonlinear structure modelling for reinforced concrete (RC) and steel-composite (SC) structure requirements in the Japanese JEAC 4601-2015/4618-09 and AIJ RC 2018 standard, or in the US and ASCE 4-16 and ACI 318-19/ACI 349-13/AISC N690-18 standards.

Independent verification and validation studies against experimental testing (NUPEC data) and rigorous nonlinear time domain analysis (based IAEA KARISMA multiyear project) indicated that the iterative SSI equivalent-linearization procedure implemented in the ACS SASSI Option NON provides a reasonable accuracy and a very high numerical efficiency (Ichihara et al., 2022, Nitta e al., 2022).

DEEPLY EMBEDDED SMR CASE STUDY

The reinforced concrete (RC) SMR structure has a footprint dimensions of 100 ft by 100 ft, and has a total height of 162.50 ft including 118 ft embedment. The exterior and containment walls are 3 ft thick, while the interior compartment walls are 2 ft thick. The SMR SSI model is described in Figures 1 and 2. The has a total of 30,924 nodes including 15,780 excavation nodes. The interaction nodes were defined for all excavation volume outer nodes, plus 11 internal node layers (red dots). out of the total of 30 internal node layers in the excavation, respectively.

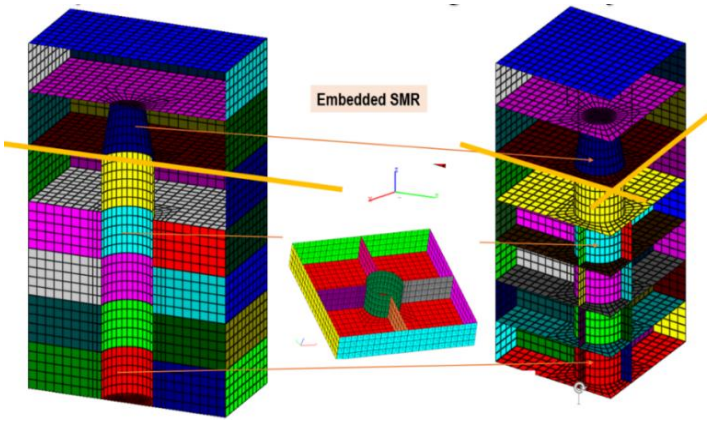

Figure 1 SMR Structure FE Model Description (left plots) including ISRS Output Locations (right plot)

The generic soil site condition was defined were by an uniform deep soil deposit with Vs=1,500 fps. The nonlinear wall-soil interface slipping was modeled using distributed nonlinear shear springs at the SMR wall-soil interface. The nonlinear springs have bilinear force-displacement relationships that depend on the geological static soil pressure variation with depth. The slipping forces (yielding level) correspond to the friction forces at the wall-soil interface which vary with depths up to the soil shear stress upperbound of 2 ksf (limit value per API standard) which corresponds to about a depth of about 35 ft.

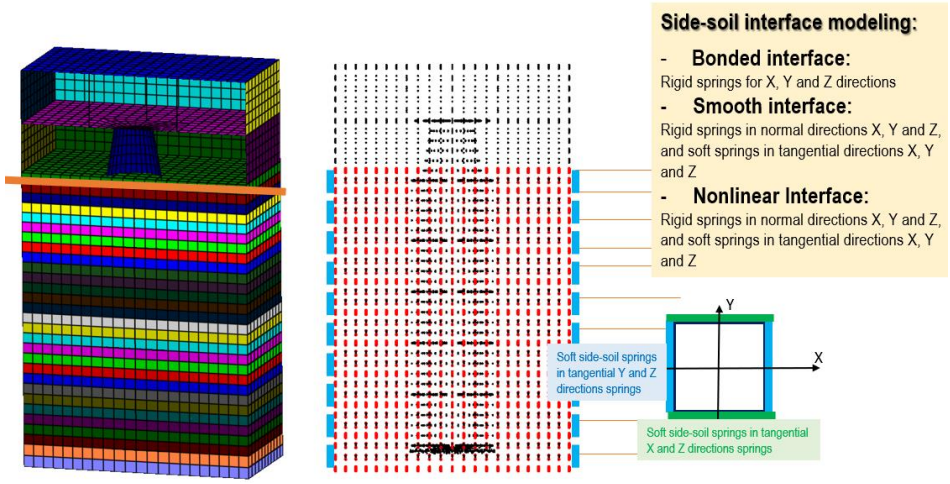

Figure 2 SMR SSI Model; FE Model Mesh (left), Nodes (middle) and Soil-Interface Modeling (right)

The seismic input at the ground surface was defined by the RG1.60 seismic input with a 0.6g maximum acceleration, which is well-above design level input. The input control motion for the SSI analysis was defined at the SMR foundation level by the in-column soil motions.

The seismic incoherent motion inputs were defned based on the Abrahamson coherence functions for soil sites (Abrahamson, 2007). Figure 3 illustrates a qualitative comparison between the coherent (1D waves) and the incoherent (3D waves) seismic soil motions. Figure 3 (right) shows a three-dimensional view of the soil surface motion under coherent and incoherent seismic waves. Simulated incoherent motions were generated based on the Abrahamson stochastic modelling of the spatially varying motions assuming isotropic coherence functions (same coherence in all directions).

In addition to the Abrahamson plane-wave coherency modelling for soil sites, an apparent traveling wave speed of 10,000 fps was also included along the X-input horizontal direction.

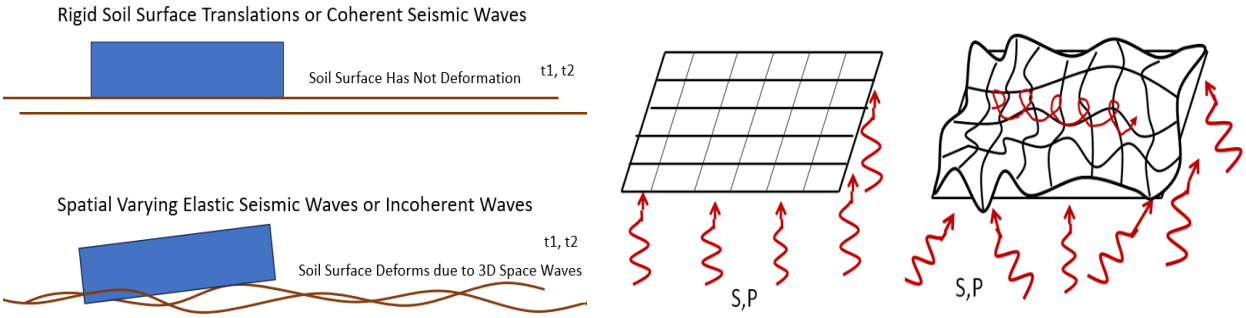

Figure 3 Qualitative Comparison Between Coherent and Incoherent Motion Inputs

All incoherent SSI analyses were performed using the ACS SASSI Stochastic Simulation (SS) approach. The SS approach uses a rigorous Monte Carlo simulation for generating the incoherent stochastic seismic wavefields based on the Abrahamson coherency soil models. Ten seismic input accelration wavefields were considered to compute incoherent SSI responses. The incoherent SSI responses were computed by the mean of the simulated responses.

The SSI analyses were performed using the highly efficient Flexible Volume Reduced-Order Modelling approach with soil impedance interpolation (FVROM-INT) as described elsewhere (Ghiocel, 2022, Sato et al., 2024). Hashemi has shown that the application of the ACS SASSI FVROM-INT approach to deeply embedded SMR SSSI models cut the cost of SSI analysis by up 50 times in comparison with standard SASSI analysis (Hashemi et al., 2024).

NONLINEAR STRUCTURE MODELING PER JAPAN AND US ENGINEERING PRACTICES

For the SMR structure with RC walls, the structural modelling was based on the JEAC 4601 structural modelling recommendations. The RC wall back-bone curve (BBC) equations for the nonlinear SSI analysis were computed using the JEAC 4601 Appendix 3.7 equations or ACI 318-19 equations (Ghiocel et al, 2022a, 2022b, Sato et al., 2024).

The RC wall nonlinear modelling included two major constitutive components (Figure 4):

1. Back-bone curves (BBC) for in-plane shear and in-plane bending deformation for each RC wall at each floor level per standard equations or available experimental tests (left plot, red line)
2. Hysteretic models (HM) for in-plane shear and in-plane bending cyclic deformation effects for each RC wall panel defined per standard recommendations or available experimental tests (left plots, blue loops).

The RC wall BBCs and their associated hysteretic models were determined using ACS SASSI Option NON based on the requirements of the JEAC 4601-2015 App.3.7 or ACI 318-19. Therefore, for JEAC 4601 application, the “PO shear” and “PODT bending” maximum point-oriented hysteretic models (Figure 4) were applied, as required by the standard, while for ACI 318/ASCE 4 application, the Cheng-Mertz shear and bending models, CMS and CMB, were used (Cheng and Mertz, 1989). The Cheng-Mertz models were used for decades being validated by a series of the RC wall experimental tests including the LANL and NCKU Taiwan laboratories. Dr. Mertz employed the Cheng-Mertz hysteretic models over decades at the DOE SRS research center during 1990s and later for various background studies in support of the ASCE 4 and 43 standard development. A recent validation of the Cheng-Mertz models was completed based on the NUPEC experimental test data (Ichihara, 2022).

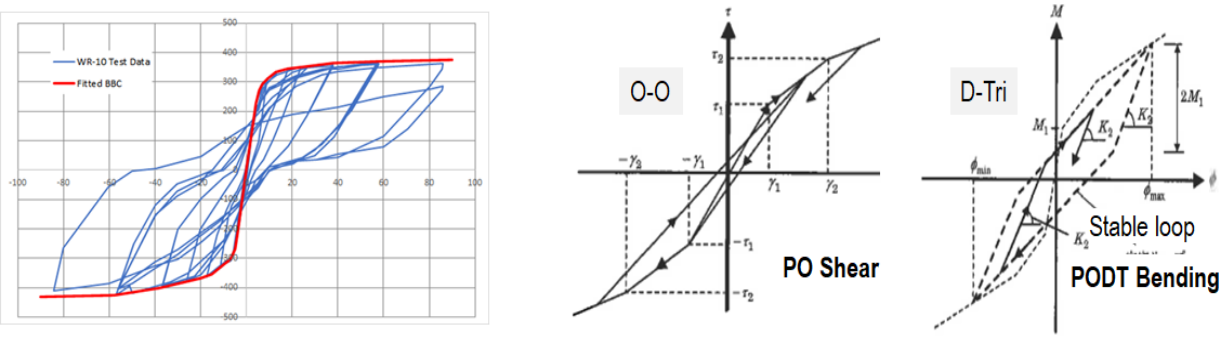

Figure 5 BBC and JEAC 4016 Recommended Maximum Point-Oriented Hysteretic Models

For nonlinear structure SSI analysis, an iterative hybrid frequency-time approach was used for performing an efficient nonlinear structure SSI analysis. The hybrid approach at each iteration includes two coupled analysis steps (Figure 6):

Step 1: An equivalent-linear SSI analysis in complex frequency via the SASSI approach to compute the structural displacements for each nonlinear RC wall, and then,

Step 2: A nonlinear time-domain hysteretic analysis for each RC wall loaded with the SSI displacements from Step 1, to compute the in-plane shear and bending nonlinear wall responses using the *standard-based back-bone curve (BBC) equations* and *appropriate hysteretic models from software library*.

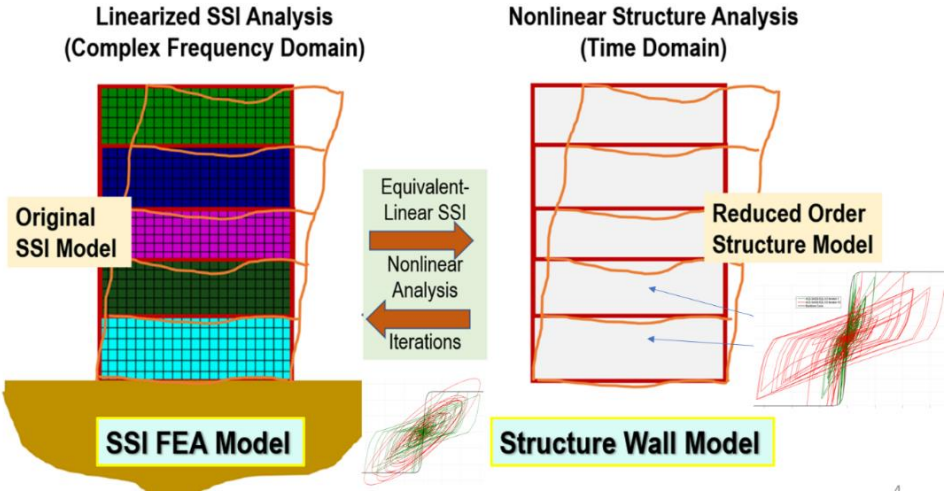

Figure 6 Fast Iterative Hybrid Nonlinear SSI Approach Implemented in ACS SASSI Option NON

It should be noted that *Step 1* uses the *original, refined FE SSI model* (left plot) while *Step 2* uses a *reduced-order structural model* (right plot) using macro-mechanics models for simulating the RC wall hysteretic behaviour. These macro-mechanics models are called wall "panels" and include groups of the shell elements defining the RC wall geometry at each floor level (see panels with different colours in Figure 9 left plot). Based on reduced-order modelling, the Step 2 nonlinear time-domain hysteretic analysis is extremely fast.

There are two hysteretic type behaviours for a RC wall panel at each iteration: 1) Shear hysteretic behaviour and, 2) Bending hysteretic behaviour. For general cases, for which the shear and bending deformation effects are both significant, the interaction between the hysteretic shear and bending effects can be

incorporated for each wall panel at each iteration assuming either ellipsoidal shaped interaction curves or orthotropic materials, as described in the ACS SASSI user manual.

Figures 7 and 8 show the shear BBC and the bending BBC based on JEAC 4601-2015/AIJ RC 2018 and ACI 318-19/ASCE 4-16, respectively, for the SMR external and cylindrical containment RC walls for all floors (see Figure 1).

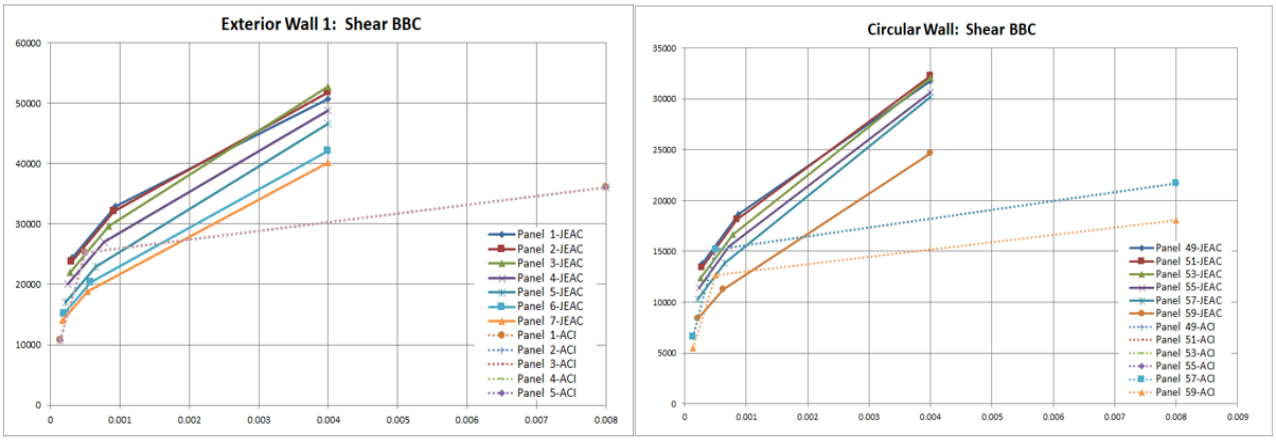

Figure 7 Shear BBCs for SMR External RC Wall (left) and Interior Containment RC Wall (right)

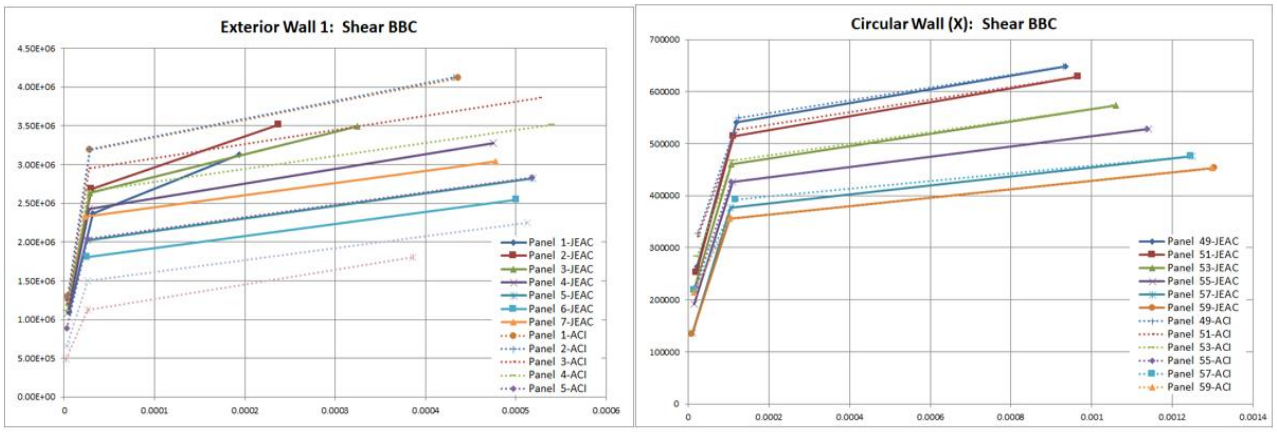

Figure 8 Bending BBCs for SMR External RC Wall (left) and Interior Containment RC Wall (right)

It should be noted that shear BBC based on JEAC standard are much higher for the ultimate point computed based on ACI standard. Explanation could be related to the lab test results used for validations, which for Japan standard include massive RC walls with strong flanges as existing in nuclear structures, including also closed box sections as described in the ACS SASSI user manual based on the original Taitokui report in Japanese (Taitokui, 1987).

It should be noted that the ACI 318-19 RC wall shear capacity equations do not include the bending moment and axial force interaction effects on the shear force capacity. In contrast, JEAC 4601includes these interaction effects (Sato, 2024).

The RC wall bending BBC capacities for external wall (including one-sided flanges) using ACI 318 are lower at the upper floors due to the reduced effective flange widths computed based on the standard for the top floors. The RC wall flanges are computed quite differently in the two standards.

COMPARATIVE OF SEISMIC SSI RESPONSES

Comparative SSI responses include the computed ISRS and exterior wall forces and moments in the deeply embedded SMR structure subjected to coherent and incoherent input motions. Figures 9 shows the locations where ISRS and the wall forces/moments were computed. The right plot shows the selected shell element lines for the SMR exterior wall for which the membrane forces and bending moments were computed. Column 3 includes a vertical middle line of shell elements (from 42 ft roof elevation down to -116 ft basemat elevation), while Columns 4 and 5 include two adjacent horizontal shell element lines from left edge to right edge below and above ground surface level.

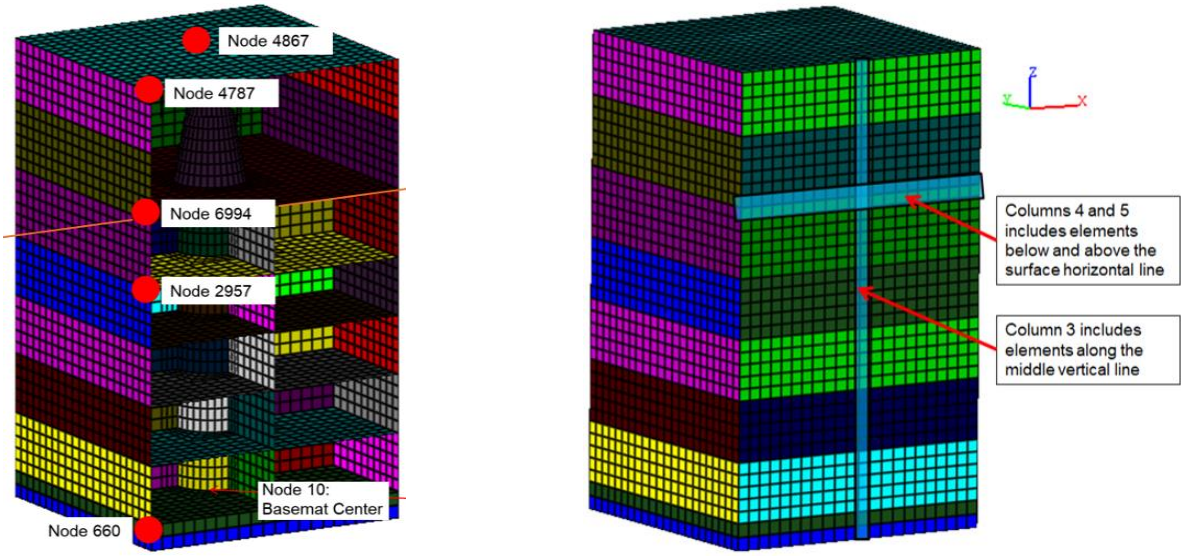

Figure 9 Selected ISRS Locations (left) and Shell Element Lines for SMR Wall Forces (right)

Linear SSI Coherent and Incoherent Results

The initial comparisons were done for the elastic linear SSI analysis results assuming either a smooth and a bonded wall-soil slipping interface. These comparisons are shown in Figures 10, 11 and 12. Figures 10 and 11 show the incoherent and coherent ISRS at the SMR external wall corner at the ground surface level at 0 ft elevation (Node 6994), and below the ground surface level at the SMR basement center at 30 ft elevation (Node 9183). Figure 10 shows horizontal ISRS and Figure 11 shows vertical ISRS.

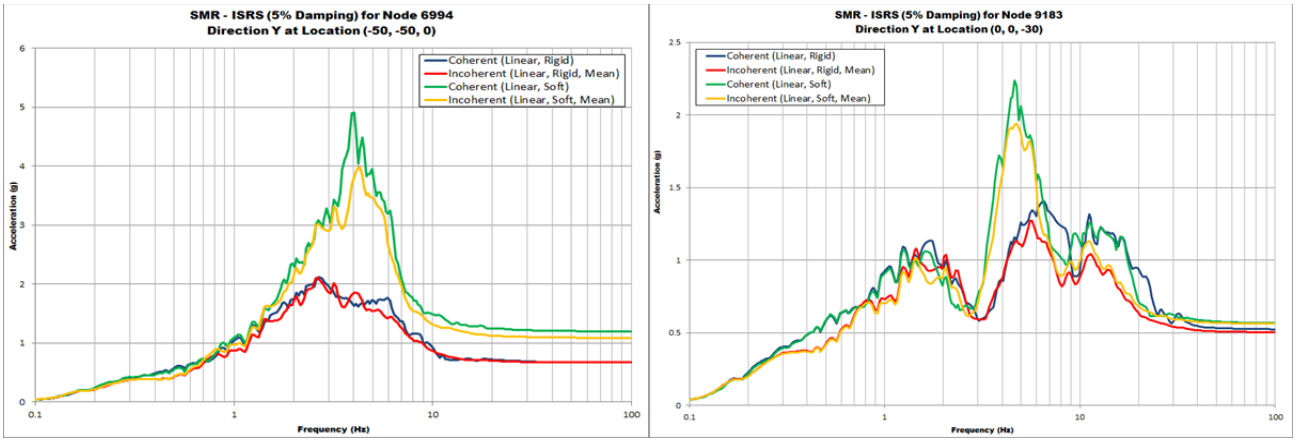

Figure 10 Horizontal SMR ISRS at at Ground Surface, El. 0 ft, and Below Ground Surface, El. -30ft

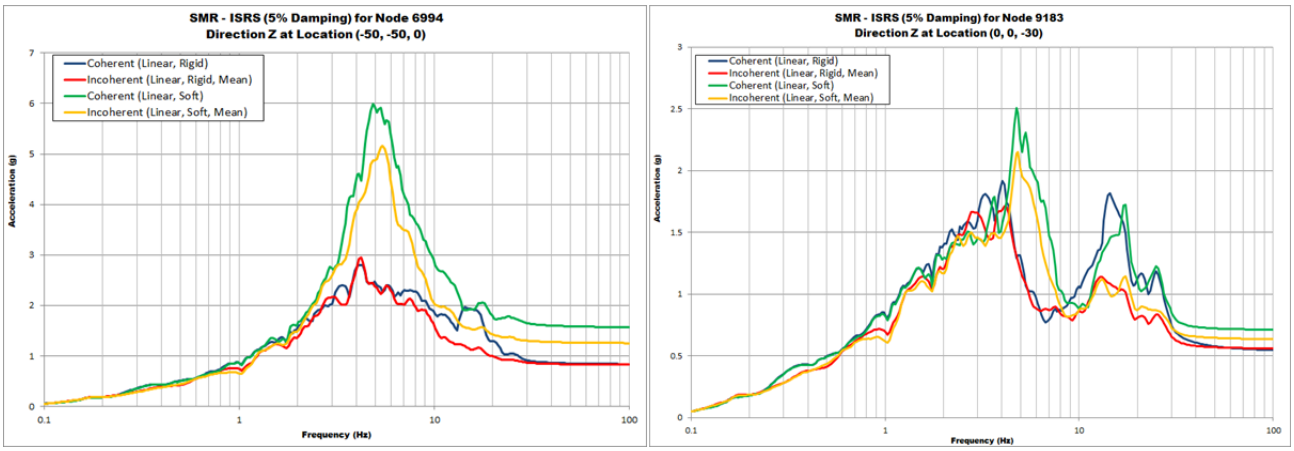

Figure 11 Vertical SMR ISRS at Ground Surface, El. 0 ft, and Below Ground Surface, El. -30ft

The above comparative results indicate that the ISRS computed for the smooth interface assumption are much larger than ISRS computed for the bonded interface. As expected, for the investigated SMR structure with a relatively horizontal section area of 100 ft x 100 ft, the motion incoherency effects on ISRS are quite reduced and also favourable.

Figure 12 compares the in-plane and out-of-plane maximum shear forces in the SMR exterior wall along the Column 3 vertical line of shell elements (from roof elevation to basemat elevation).

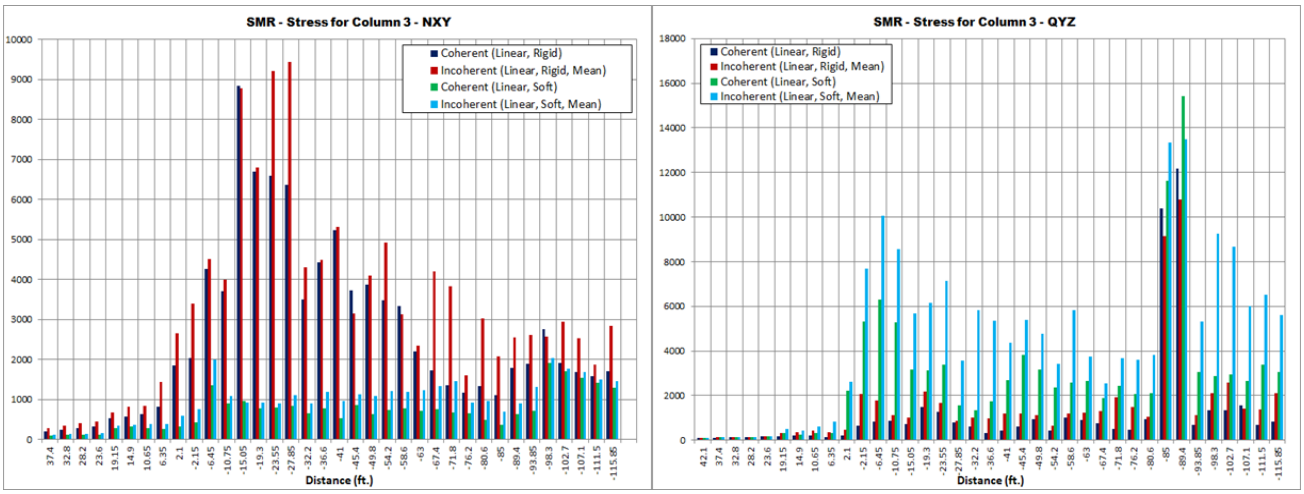

Figure 12 Maximum In-Plane and Out-of-Plane Shear Forces (NXY and QYZ) in Exterior SMR Wall

Results show that the bonded interface assumption produces much larger in-plane NXY shear forces and much smaller transverse QYZ shear forces than the smooth interface assumption. The motion incoherency effects in the SMR wall forces are significant, but these effects are less drastic than the effects due to the assumed wall-soil interface condition.

Linear vs. Nonlinear SSI Coherent Results

In this section the linear SSI and nonlinear SSI results for coherent input motion are compared. For nonlinear SSI analysis, the structural modelling was made based on the JEAC 4601-15 and ACI 318-19 standards.

Figures 13 and 14 compare the linear and nonlinear ISRS results for coherent inputs. Only the smooth soil interface assumption was considered for these linear SSI in these comparisons. Nonlinear SSI analysis included the nonlinear wall-soil interface slipping effects. Figure 13 shows the ISRS at the SMR wall corner at ground surface level (Node 6994), and Figure 14 shows the transverse (QYZ) and in-plane (NXY) shear forces in the SMR wall shell elements along the Column 3 vertical middle line of shell elements from the roof to foundation basemat levels (see Figure 9 for output location).

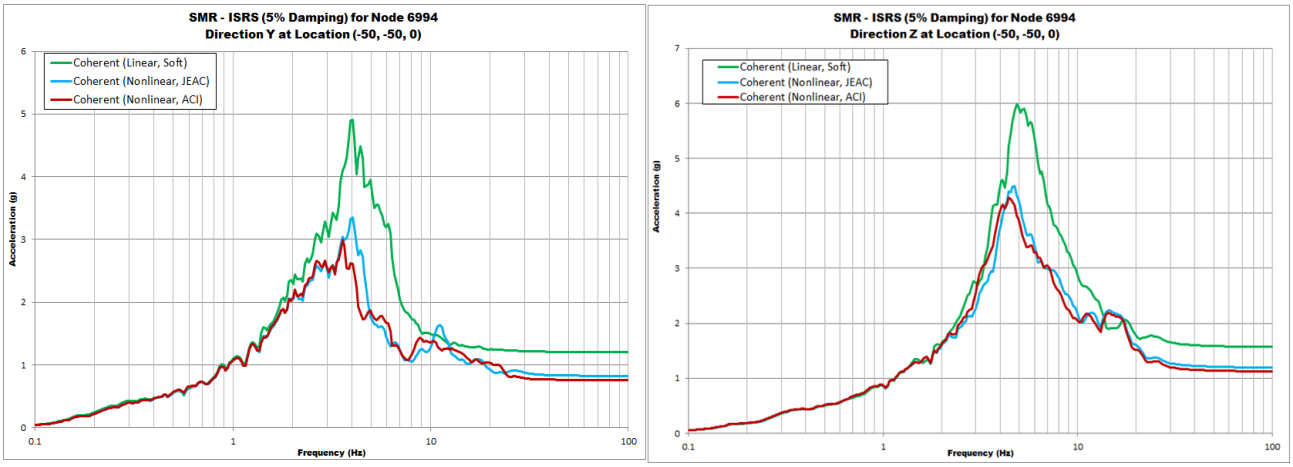

Figure 13 Linear & Nonlinear Coherent ISRS Based on JEAC 4601 and ACI 318 for Y-Dir and Z-Dir

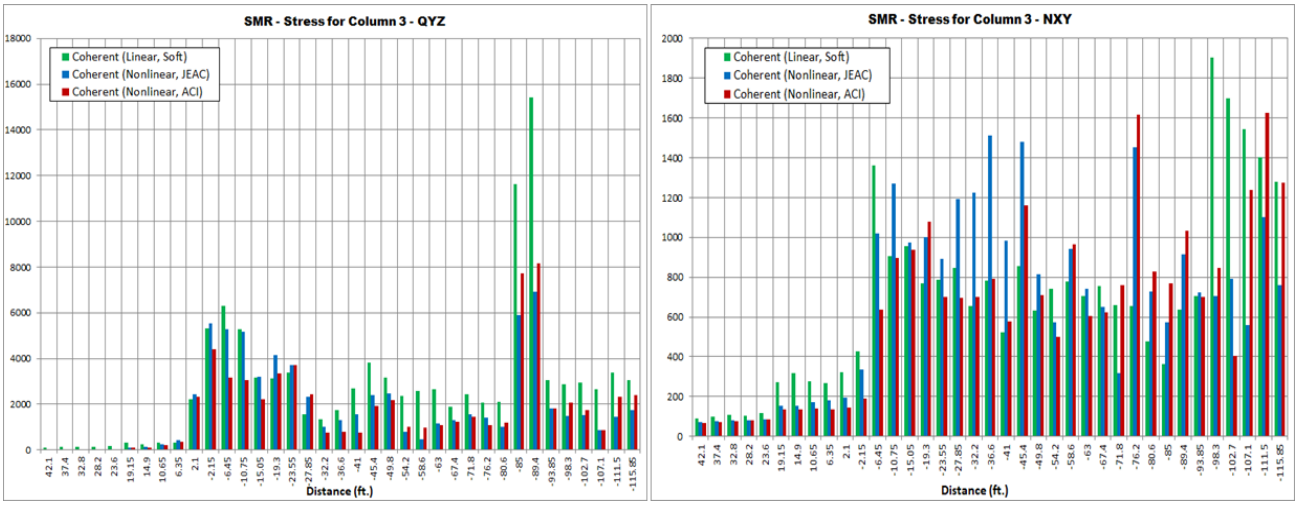

Figure 14 Linear & Nonlinear Coherent Shear Forces, QXZ and NXY, Based on JEAC 4601 and ACI 318

The coherent SSI results in Figures 13 and 14 indicate that linear SSI analysis with assumed smooth soil interface provides larger ISRS and transverse QYZ element shear forces in SMR wall than nonlinear SSI analyses. However, for the in-plane NXY element shear forces, linear SSI analyses could provide either smaller or larger forces in the SMR wall.

It should be noted that SMR wall forces computed using the JEAC 4601 and the ACI 318 standards for nonlinear structural modelling could be quite different, as shown Figure 14 for the NXY shear force diagram along a wall vertical middle line of shell elements.

Figure 15 shows the in-plane nonlinear hysteretic shear forces and bending moments in the SMR exterior wall panel for the sixth floor or first floor above ground surface level (Panel 6) for the two assumed linear

wall-soil interface conditions, smooth and bonded, instead of considering the nonlinear interface behaviour. Therefore, in Figure 15, only nonlinear structure behaviour is considered based on the JEAC 4601 and thee ACI 318 standards. As shown, the bonded interface condition (rigid tangential springs) provides much larger in-plane nonlinear shear forces and bending moments in the SMR wall than the smooth interface condition (extremely flexible tangential springs).

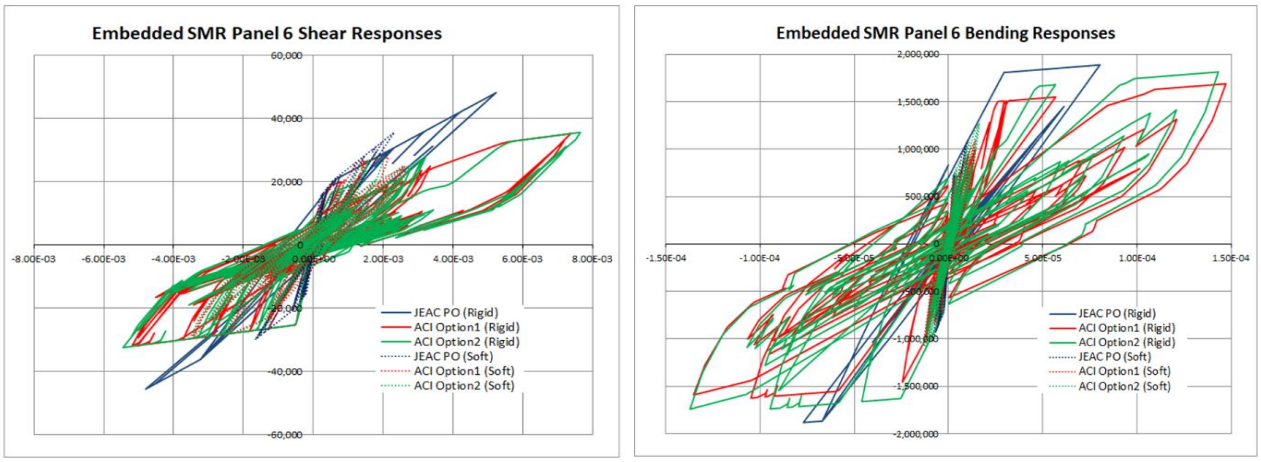

Figure 15 Shear Force (left) and Bending Moment (right) Nonlinear Hysteretic Responses of SMR Exterior Wall at the 1st Floor Above Ground Surface (Panel 6 at sixth floor level)

Figure 15 results are consistent with previous observations for the linear SMR SSI results in Figure 12 (left plot) for the NXY element shear forces in SMR wall which were much larger for the bonded interface.

Nonlinear SSI Coherent and Incoherent Results

In this section the nonlinear SSI results computed for coherent and incoherent input motions are compared. For nonlinear SSI analysis, the structural modelling was based on the JEAC 4601-15 and the ACI 318-19 standards, and also included the nonlinear wall-soil interface slipping effects.

Figure 16 shows the incoherent and coherent nonlinear ISRS in horizontal and vertical directions at the SMR basement center below the ground surface level at -30 ft elevation (Node 9183). Figure 17 shows incoherent and coherent nonlinear ISRS in horizontal direction at the SMR wall corner at the ground surface level at elevation of 0 ft (Node 6994) and at the SMR roof level at elevation of 44.5 ft (Node 4787).

Figures 16 and 17 indicate that coherent ISRS (solid lines) are larger than incoherent ISRS (dashed lines) below ground surface level at SMR center location and smaller above the ground surface at corner locations. Figure 17 results suggests that the horizontal nonlinear ISRS computed at the SMR wall corner includes some torsional effects induced by motion incoherency. The largest difference is reached at the SMR roof corner where incoherent ISRS are 30-40% larger than coherent ISRS. It should be also noted that the nonlinear ISRS computed based on the JEAC 4601-15 and the ACI 318-19 standards are quite close.

The nonlinear SSI results are qualitatively different than the linear SSI results, as can be noted if the linear ISRS results in Figure 13 are compared with the nonlinear ISRS results in the Figure 17 for the Node 6994 location. However, it worth noting that the nonlinear incoherent ISRS, which are larger than nonlinear coherent ISRS, are still less when compared with the linear coherent ISRS. For the Node 6994 location, the ISRS peak amplitude is 4.91g for linear SSI and only 3.75g for nonlinear SSI. This indicate that for the investigated linear SSI analysis is a conservative approach for computing ISRS.

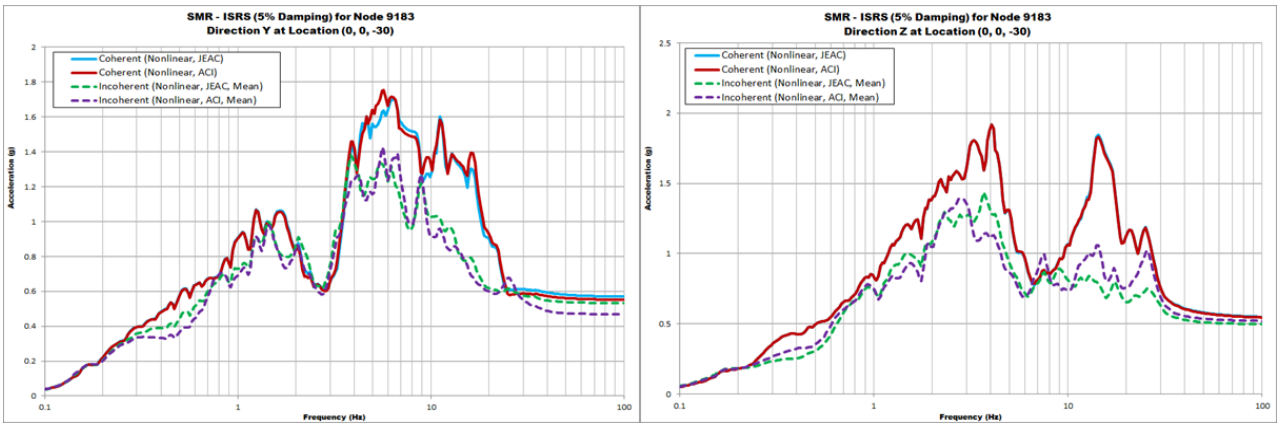

Figure 16 Nonlinear ISRS at Floor Center at -30 ft Below Ground Surface; Y-Dir (left) and Z-Dir (right)

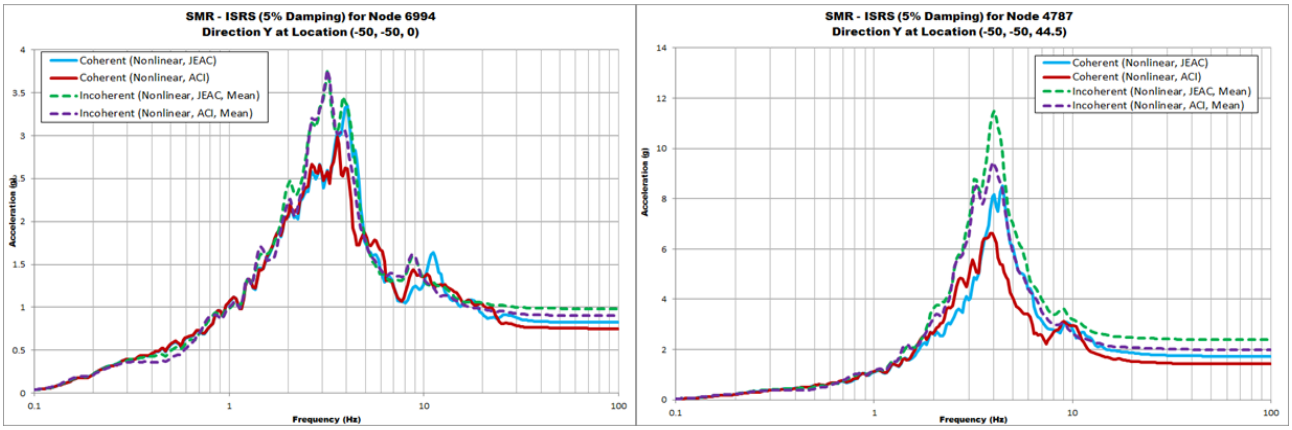

Figure 17 Nonlinear ISRS at SMR Wall Corner at Ground Surface (left) and Roof Level (right) in Y-Dir

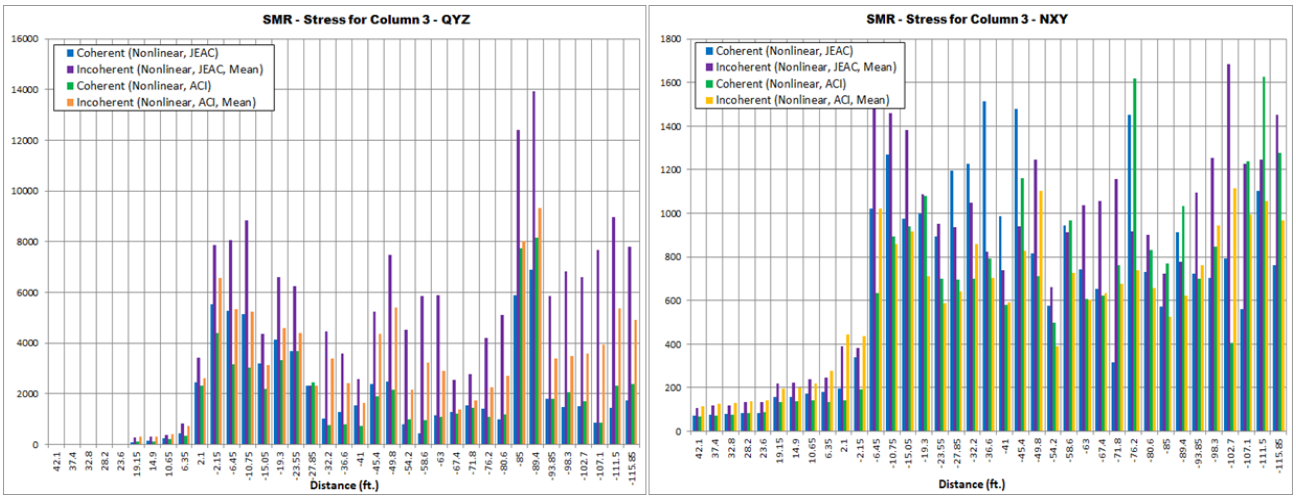

Figure 18 Coherent and Incoherent Transverse QYZ and In-Plane NXY Shear Forces Along Column 3 of Vertical Line of Shell Elements from Roof Elevation of 42.1 ft to Foundation Elevation of -115.85 ft

Figure 18 compares the coherent and incoherent QYZ and NXY shear forces in SMR wall for the Column 3 vertical middle line from roof to foundation levels (see Column 3 line location in Figure 9). The transverse

QYZ shear force diagram shows much larger values for the incoherent motions than the coherent motions as result of the differential soil motions produced by incoherent waves at the wall-soil interface that increase the kinematic SSI effects on the SMR walls. For in-plane NXY shear force diagram, the incoherent response is still larger than coherent response, but not this is not applicable to all depths below ground surface.

It should be also noted that the QYZ and NXY nonlinear shear forces computed based on the JEAC 4601 recommendations are significantly larger than those based on the ACI 318 recommendations (see BBC in Figure 7). Significant differences between the results obtained based on the two standards application are also noted for the QYZ and NXY forces. For the transverse QYZ shear forces, the incoherent motions produced much higher results than the coherent motions, and the JEAC 4601-based results are significantly larger than ACI 318-based results.

CONCLUDING REMARKS

The paper investigates the effects of coherent and incoherent motions on the nonlinear structure behaviour for a typical deeply embedded SMR structure. The nonlinear SSI approach follows conceptually the Japanese structure modelling and seismic engineering practices. Specifically, the implementation is compliant with the nonlinear structure modelling for reinforced concrete (RC) and steel-composite (SC) structure requirements in the Japanese JEAC 4601-2015/4618-09 and AIJ RC 2018 standard, or in the US and ASCE 4-16 and ACI 318-19/ACI 349-13/AISC N690-18 standards.

Linear and nonlinear SSI analysis results were also compared. No SSSI effects were considered herein. The seismic SSSI effects which can largely affect deeply embedded SMR responses were investigated elsewhere (Ghiocel and Todorovski, 2024).

For the investigated deeply embedded SMR structure the motion incoherency effects are larger for the seismic stress demands than ISRS. The kinematic SSI effects are larger for incoherent motions due to the soil differential motions in horizontal plane at different depths. As shown, an important factor that could significantly affect kinematic SSI effects and increase SMR embedded wall forces is the wall-soil interface condition. For linear SSI analysis, two bounding conditions, specifically, no-friction, smooth wall-soil interface and fully-welded, bonded wall-soil interface were considered. For nonlinear SSI analysis, the wall-soil interface slipping is nonlinearly handled using shear stress-dependent friction springs.

For the selected uniform firm soil site and RG1.60 spectrum input, the coherent nonlinear ISRS appear be higher than the incoherent nonlinear ISRS at the lower elevations below ground surface and the SMR center locations, but visibly lower at higher elevations above ground surface and the SMR wall corner locations. The largest differences are computed at the SMR roof corners where the incoherent ISRS can be up to 30-40% larger than the coherent ISRS. These results are highly dependent on the site-specific conditions, potentially including higher frequency content inputs and nonuniform soil profiles, on a case-by-case basis.

For the investigated deeply embedded SMR case study, the comparative ISRS results for linear SSI analysis (with smooth wall-soil interface) and nonlinear SSI analysis (with nonlinear wall-soil interface) indicated that the linear SSI analysis is conservative. It should be noted that this is consistent with US practice based on linear SSI analysis for deeply embedded SMR, in accordance with ASCE 4-16 for RC structures and AISC N690-18 for SC structures.

REFERENCES

Abrahamson, N. (2007). Abrahamson, N. (2007). Effects of Spatial Incoherence on Seismic Ground Motions, *Electric Power Research Institute, Palo Alto, CA and US Department of Energy, Germantown, MD, Report No. TR-1015110,* December

American Concrete Institute (2020), Building Code Requirements for Structural Concrete and Commentary, *ACI 318-19 Standard*

American Society of Civil Engineers (2017), Seismic Analysis for Safety-Related Nuclear Structures and Commentary, *ASCE 4-16 Standard*

Cheng, Y.F. and Mertz, G. (1989). Inelastic Seismic Response of Reinforced Concrete Low-Rise Shear Walls of Building Structures, *University of Missouri-Rolla, Civil Engineering, CE 89-30*

Ghiocel, D.M.(2022). Efficient Linear and Nonlinear Seismic SSI Analysis of Deeply Embedded Structures Using Flexible Volume Reduced-Order Modelling (FVROM), *SMIRT26 Conference, Division V*, Berlin/Potsdam, Germany, July 10-15

Ghiocel, D.M. and Todorovski, L. (2024) Seismic SSSI Analysis for Deeply Embedded SMR Structure Founded on Different Nonuniform Soil Site Conditions, *SMIRT27 Conference, Division V*, Yokohama, Japan, March 3-8

Ghiocel, D.M, Nitta, Y. and R. Ikeda, T. Shono (2022). Seismic Nonlinear SSI Approach Based on Best Practices in US and Japan. Part 1: Modelling, *SMiRT26, Special Session on Nonlinear Seismic SSI Analysis Based on Best Practices in US and Japan*, Berlin, July 10-15

Ghiocel, D.M, Nitta, Y. and R. Ikeda, T. Shono (2022). Seismic Nonlinear SSI Approach Based on Best Practices in US and Japan. Part 2: Application, *SMiRT26, Special Session on Nonlinear Seismic SSI Analysis Based on Best Practices in US and Japan*, Berlin, July 10-15

A-AA, NON, PRO, RVT-SIM and UPLIFT, Revision 7, Rochester, NY, January 31

Ghiocel, D.M. and Saremi, M., (2017). Automatic Computation of the Strain-Dependent Concrete Cracking Pattern for Nuclear Structures for Site-Specific Applications", *the SMiRT24 Conference, Division V, Paper 408, Busan*, Korea, August 20-25

Ghiocel Predictive Technologies (2023) ACS SASSI NQA Version 4.3 An Advanced Computational Software for 3D Dynamic Analysis Including Soil-Structure Interaction, *GP Technologies, Inc., User Manuals, Revision 9*, Pittsford, New York

Hashemi, A., Elkhoraibi, T., Ghiocel, D.M. and Todorovski (2024) "Site-Specific SSSI Analysis for Deeply Embedded SMR Using Flexible Volume Reduced-Order Modelling with Impedance Interpolation (FVROM-INT)", *SMiRT27 Conference, Division V, Yokohama*, March 3-8.

Ichihara, Y., Nakamura, N, Nabeshima, K., Choi, B. and Nishida, A. (2022). Applicability of Equivalent Linear Three-Dimensional FEM Analysis for Reactor Building to Seismic Response of Soil-Structure Interaction System, *SMiRT26 Conference, Special Session on Nonlinear Seismic SSI Analysis Based on Best Practices in US and Japan*, Berlin, July 10-15

Nitta, Y., Ikeda, R., Horiguchi, T. and Ghiocel, D.M. (2022). Comparative Study Using Stick and 3DFEM Nonlinear SSI Models per JEAC 4601-2015 Recommendations, *SMiRT26, Special Session on Nonlinear Seismic SSI Analysis Based on Practices in US and Japan*, July 10-15

Nuclear Standard Committee of Japan Electric Association (2015), *Technical Code for Aseismic Design of Nuclear Power Plants*, Japan Electric Association Code (JEAC 4016-2015)

Sato, Y., Ghiocel, D.M., Kataoka, S., Morimoto, Y. (2024). "Study on Fluid-Structure-Soil Interaction (FSSI) Effects for A Deeply Embedded Nuclear Facility with A Large-Size Pool Under Severe Earthquake. Part 2: Nonlinear SSI", *SMiRT27 Conference, Division V*, Yokohama, March 3-8

Taitokui, M. (1987). *Restoring Force Characteristics for RC Structure Walls* (in Japanese), Technical Report for Architectural Institute of Japan and Japan Atomic Energy Agency.